Optics & Laser Technology 88 (2017) 161–165

Contents lists available at ScienceDirect

Optics & Laser Technology

journal homepage: www.elsevier.com/locate/optlastec

Spectral optimization based simultaneously on color-rendering index and color quality scale for white LED illumination

J.J. Zhang[a,b], R. Hu[a], X.J. Yu[a], B. Xie[a], X.B. Luo[a,*]

[a] School of Energy and Power Engineering, Huazhong University of Science and Technology, Wuhan, Hubei 430074, PR China
[b] School of Automation, China University of Geosciences, Wuhan, Hubei 430074, PR China

ARTICLE INFO

Keywords:
Light-emitting diodes
Spectral optimization
Color rendering
Color temperatures

ABSTRACT

Color performance is an important parameter for high-quality light-emitting diode (LED) lighting. Color-rendering index (CRI) and color quality scale (CQS) are two independent parameters to assess the color performance, but high CRI does not correspond to high CQS, and vice versa. Therefore, it's urgent to find a comprehensive and effective metric for assessing the color performance of LEDs that can simultaneously exhibit high color-rendering index (CRI) and high color quality scale (CQS) values. In this study, a genetic algorithm with a penalty function was proposed for realizing spectral optimization by boosting the maximum attainable luminous efficacy of radiation (LER) of spectra while constraining both high CRI and CQS. By simulations, white spectra from LEDs with CRI≥95 and CQS≥95 were achieved at different correlated color temperatures (CCTs) from 2020 K to 7929 K. Further, a real spectra-tunable LED module consisting of four LEDs is fabricated, and high LER (344 lm/W) and color performance (CRI≥90, CQS=90) was realized by tuning driving currents.

1. Introduction

White light-emitting diodes (LEDs) have been developing rapidly since the first blue LED was created in 1986 [1,2]. White LEDs offer great market potential for general illumination applications because of their merits: long lifetime, environmental friendliness, and high luminous efficiency [3]. However, white LEDs still suffer from challenges related to color quality, including color rendering, color preferences, and gamut area performance, which are other measures of vital performance in addition to luminous efficacy.

The color-rendering index (CRI) [4] was developed in the last century for assessing the color fidelity of the then-new fluorescent lamps [5]. However, the recent development of LED sources exposes some shortcomings of the CRI. For example, its color space is not uniform and color samples are low saturated [5,6]; therefore, LEDs with high CRIs may render high saturated objects very poorly. Several deficiencies and limitations appear when assessing the color rendering of white LEDs, especially for white LEDs with strong peaks and pronounced valleys in their spectra [7]. Consequently, Davis and Ohno proposed the color quality scale (CQS) to assess the color quality of the white LEDs [7]. The CQS has proven to offer an improved tool for assessing the color performance of both red-green-blue (RGB) white LEDs and white LEDs with narrowband radiation. However, from the psychophysical experimental results reported by Pousset [8], the current CQS does not seem satisfactory in every aspect and requires further improvements. At this point, there is no comprehensive and effective metric for assessing the color performance of LEDs; therefore, for more comprehensive color performance, it is better to fabricate LEDs with simultaneously high CRI and CQS values than LEDs with high CRI or CQS values that vary independently [9–11]. Oh et al. [12] fabricated LEDs with high CRI and CQS values by engaging in exhaustive experimental trials, which need to be improved further by proposing and testing a numerical simulation method. In addition, Dai [13], Bulashevich [14], Zhong [15], and Davis [16] proposed spectra optimization algorithms that optimized CRI or CQS values independently. Further, the problem of optimizing CRI and CQS values simultaneously is complicated by the connections and conflicts between luminous efficacy of radiation (LER), CRI, and CQS. Consequently, there is an urgent need for proposing and testing an easy and effective spectral optimization method to achieve spectra with maximal LER, including both high CRI and CQS values.

In this study, a relative spectral power distribution (SPD) model of a white LED with blue, green, yellow, and red color components was developed. A genetic algorithm (GA) with penalty functions was proposed to achieve white spectra with maximal LER and high CRI and CQS values. Then, through numerous simulations, optimal spectra of the LED were obtained at different correlated color temperatures (CCTs). Finally, a LED module consisting of four color LEDs is

* Corresponding author.
E-mail address: luoxb@hust.edu.cn (X.B. Luo).

http://dx.doi.org/10.1016/j.optlastec.2016.08.006
Received 19 May 2016; Accepted 24 August 2016

proposed. High LER and color performance were realized by tuning currents of the four LEDs.

2. Spectral optimization method

To achieve high CRI and CQS values, most sources in the literature report fabricating yellow-phosphor-converted white LEDs integrated with red phosphor, red chromatic LEDs or semiconductor colloidal quantum dots [9–11]. Therefore, our spectral model of white LEDs consists of blue chips (narrowband radiation), green and yellow phosphors (broadband radiation), and red chips or quantum dots (narrowband radiation). The relative SPD of white LEDs, $S_W(\lambda)$, is given by

$$S_W(\lambda) = p_b S(\lambda, \lambda_b, \Delta\lambda_b) + p_g S(\lambda, \lambda_g, \Delta\lambda_g) + p_y S(\lambda, \lambda_y, \Delta\lambda_y) + p_r S(\lambda, \lambda_r, \Delta\lambda_r), \quad (1)$$

where $S(\lambda, \lambda_b, \Delta\lambda_b)$, $S(\lambda, \lambda_g, \Delta\lambda_g)$, $S(\lambda, \lambda_y, \Delta\lambda_y)$, and $S(\lambda, \lambda_r, \Delta\lambda_r)$ refer to the relative SPDs of blue chips, green phosphors, yellow phosphors, and red chips, λ_b, λ_g, λ_y, and λ_r refer to the peak wavelengths of the blue, green, yellow, and red color components, $\Delta\lambda_b$, $\Delta\lambda_g$, $\Delta\lambda_y$, and $\Delta\lambda_r$ refer to the full widths at half maximum (FWHMs) of the blue, green, yellow, and red color components, and p_b, p_g, p_y, and p_r designate the proportions of the relative spectra of the blue, green, yellow, and red color components, respectively. The above spectral parameters, including peak wavelengths, FWHMs and proportions, comprise a 4×3 -dimensional parameter matrix. Narrowband radiation can be described as a modified Gaussian distribution, which is given by Ohno [6]. Broadband radiation is approximated by a Gaussian distribution in this analysis [17]. The FWHM of narrowband radiation varies from 20 nm to 50 nm [18], and the FWHM of broadband radiation varies from 80 nm to 120 nm [7,19]. Wavelengths for each color component vary from 380 nm to 500 nm for blue, 500 nm–550 nm for green, 550 nm–600 nm for yellow, and 600 nm–780 nm for red.

The spectral optimization method boosts the maximum attainable LER at high values of CRI and CQS and at various CCTs by varying the parameter matrix in the SPD model. In addition, it is important that the chromaticity difference from the Planckian locus on the CIE 1960 uv chromaticity diagram (D_{uv}) be smaller than 0.0054 for various CCTs [4]. Therefore, we maximize the LER under the constraints of CRI, CQS, *CCT*, and D_{uv} simultaneously. The spectral optimization problem can be described as

$$\begin{cases} Maximum: \ LER \\ Constraints: R_a \geq R_{as}, \ R_9 \geq R_{9s}, \ Q_a \geq Q_{as}, D_{uv} \leq 0.0054, \\ \qquad\qquad \dfrac{|CCT - CCT_{tar}|}{CCT_{tar}} \leq 0.01 \end{cases}, \quad (2)$$

where *LER* is the direct optimization goal, R_{as}, R_{9s}, and Q_{as} are the optimization constraints referring to the general CRI (R_a), the special CRI for strong red (R_9), and the general CQS (Q_a), respectively. Here, R_{as}, R_{9s}, and Q_{as} are assigned as 95. CCT_{tar}, the designated value of *CCT*, varies from 2000 K to 7000 K at an interval of 1000 K. In our optimization, the constraint of deviation between the actual *CCT* and CCT_{tar} is less than 1%.

In this paper, we adopted a genetic algorithm (GA) for calculating the maximum value of *LER*. Besides, penalty functions, $g_j(\vec{x})$, are used to handle the inequality constraints in Eq. (2), referring to R_a, R_9, Q_a, and *CCT* [20]. The fitness function $F(\vec{x})$ of the GA, defined as the sum of the objective function $f(\vec{x})$ and the penalty terms which depend on the constraints, can be expressed as

$$F(\vec{x}) = f(\vec{x}) + \sum_{j=1}^{5} \left(R_j \langle g_j(\vec{x}) \rangle^2\right), \quad (3)$$

where R_j, a very large positive number, is the penalty parameter of the jth constraint $g_j(\vec{x})$. The vector $\vec{x}$ of the parameter matrix that meets the constraints is defined as the feasible solution. Here, $\langle\rangle$ denotes the absolute value of the operand, if the operand is negative and returns a value zero; otherwise it returns itself and can be expressed by Eq. (4):

$$\langle g_j(\vec{x}) \rangle = \begin{cases} 0, \ g_j(\vec{x}) \leq 0 \\ g_j(\vec{x}), \ g_j(\vec{x}) > 0 \end{cases}. \quad (4)$$

In order to reduce both the mutual influence of *LER*, R_a, R_9, Q_a, D_{uv}, and *CCT* in the fitness function $F(\vec{x})$, the objective function and the penalty functions are normalized. The objective function and penalty functions can be expressed as

$$\begin{cases} f(\vec{x}) = \dfrac{683 - LER}{683} \\ g_1(\vec{x}) = \dfrac{R_a - R_{as}}{R_{as}} \\ g_2(\vec{x}) = \dfrac{R_9 - R_{9s}}{R_{9s}} \\ g_3(\vec{x}) = \dfrac{Q_a - Q_{as}}{Q_{as}} \\ g_4(\vec{x}) = \dfrac{D_{uv} - 0.0054}{0.0054} \\ g_5(\vec{x}) = \dfrac{|CCT - CCT_{tar}|/CCT_{tar} - 0.01}{0.01} \end{cases}. \quad (5)$$

As the penalty parameter R_j is a very large positive number, when R_a, R_9, Q_a, D_{uv}, or *CCT* do not meet the constraints, the fitness function $F(\vec{x})$ will be a much larger positive number than in the case when all the constraints are met. Thus, the GA evolutionary process will force the solution of the equation to approach the feasible solution that meets the constraints. The flowchart of the genetic algorithm is shown in Fig. 1.

The main processes in the GA include several steps: (1) initializing the chromosome group randomly, where the chromosome consists of the spectral proportions, the peak wavelengths, and the FWHMs; (2) calculate the fitness function of each chromosome; (3) sorting the chromosomes by fitness value and replicate the chromosomes with low fitness values to the child generation; (4) selecting two chromosomes and change their genes randomly; (5) changing a gene of a chromosome randomly, thereby producing a child generation; (6) determining whether the fitness function satisfies the stop conditions, which can be of two kinds: one is the number of evolution generations has been reached; the other is the lowest fitness function in each chromosome group does not change over 500 generations. Here, the detailed GA parameters are as follows: the number of chromosomes is 40, the precision of chromosomes is 25, the penalty parameter R_j is 2000, the generation gap is 0.9, and the probability of crossover occurring between pairs of chromosomes is 0.7.

3. Results and discussions

By conducting numerous simulations, the optimal spectral parameters of each color component and their performances with R_a, R_9, and $Q_a \geq 95$, at CCTs from 2020 K to 7929 K for maximal *LER*, have been obtained by maximizing $F(\vec{x})$. The simulation results are listed in Table 1. When CCT_{tar} is assigned values of from 2000 K to 8000 K at intervals of 1000 K, it is shown that the deviations between the *CCT* of the optimized white spectra and CCT_{tar} meet the constraints of less than 1%.

In addition, white light spectra with maximal *LER* and constrained high R_a, R_9, and Q_a are obtained by varying the value of the parameter matrix (peak wavelengths λ, FWHMs $\Delta\lambda$, and proportions p). The optimal spectrum at *CCT*=2020 K exhibits performance in which *LER*=273 lm/W, R_a=98, R_9=97, and Q_a=86. Q_a is only 86 when *CCT*=2020 K because Q_a must, in addition, be multiplied by a CCT factor which is less than 1 when *CCT* < 3500 K [7]. Therefore, 86 is a relatively high CQS at *CCT*=2020 K. In addition, *LER* reaches its

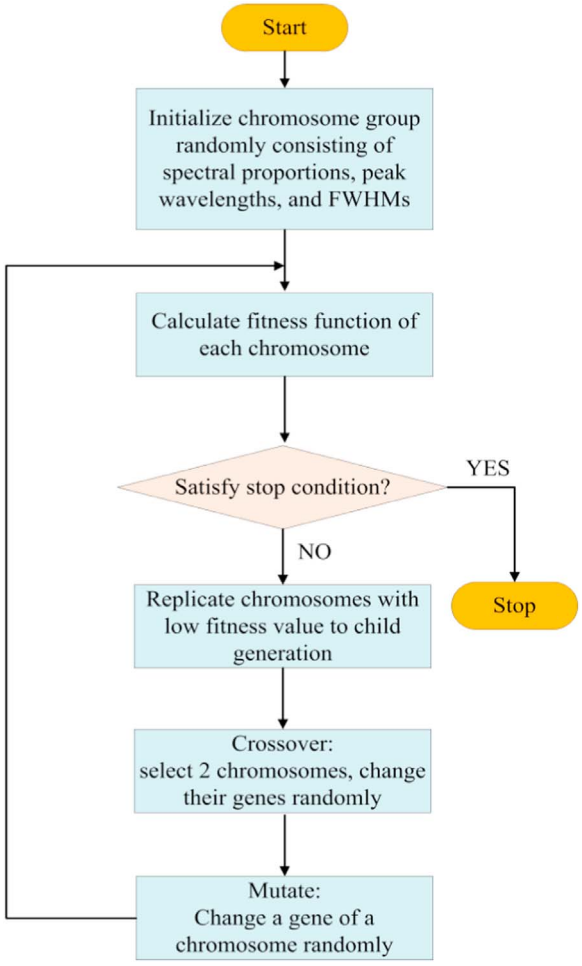

Fig. 1. GA flowchart.

Table 1
Results of simulations.

CCT_{tar}(K)	2000	3000	4000	5000	6000	7000	8000
CCT(K)	2020	2996	4014	4954	5940	6929	7929
D_{uv} (10^{-4})	17	46	7	54	26	54	51
λ_b(nm)	478.7	450.7	426.1	454.0	456.3	453.0	454.2
λ_g (nm)	515.5	532.4	508.9	523.9	506.3	503.9	500.7
λ_y (nm)	597.7	594.7	598.3	572.5	588.5	576.8	555.6
λ_r (nm)	642.1	639.8	630.3	630.9	647.1	647.5	657.2
$\Delta\lambda_b$ (nm)	34.9	33.4	32.0	38.1	20.8	31.2	50.0
$\Delta\lambda_g$ (nm)	96.6	99.8	98.4	80.0	82.4	86.7	80.0
$\Delta\lambda_y$ (nm)	115.7	88.3	116.2	101.0	116.8	101.6	120.0
$\Delta\lambda_r$ (nm)	31.9	33.1	38.7	41.9	35.6	28.3	45.0
p_b	0.46	0.52	1.00	0.63	0.72	0.63	0.74
p_g	0.00	0.15	0.86	0.93	1.00	1.00	1.00
p_y	0.06	0.39	0.98	0.72	0.75	0.69	0.26
p_r	1.00	1.00	0.96	1.00	0.60	0.85	0.79
LER (lm/W)	273	318	287	310	278	275	247
R_a	98	97	95	96	95	95	95
R_9	97	96	95	95	95	95	95
Q_a	86	96	95	96	95	97	95

highest value of 318 lm/W when CCT=2996 K. The corresponding optimal spectrum has a high color performance with R_a=97, R_9=96, and Q_a=96. The lowest LER is 247 lm/W at CCT=7929 K. Similarly, the corresponding optimal spectrum has a high color performance with R_a=95, R_9=95, and Q_a=95. Spectra with high CRI and CQS values (≥95) can be obtained at different CCTs from 2020 K to 7929 K. When compared with existing literature, when the CRI values are equal (CRI≥95), the CQS values (CQS≥95) in our method are higher than that in Ref. [21] when optimizing CRI independently (CQS≥90).

CCT-tunable white LED spectra are shown in Fig. 2(a); the color coordinates of optimized white spectra in a CIE 1931 diagram are shown in Fig. 2(b). The coordinates of the optimized white spectra are quite near the line of the blackbody radiation with the same CCTs. The chromaticity differences between them are less than 0.0054, which can be concluded from Table 1. Fig. 2 shows that the CIE x of optimized white spectra varies from 0.29 to 0.52 and the CIE y varies from 0.31 to 0.41, which yields a relatively large area of color coordinates. Therefore, the spectra optimization method for CCT-tunable LEDs can produce acceptable results for many illumination applications of different CCTs and CIE color coordinates.

Fig. 2 shows that the peak wavelengths, FWHMs, and proportions, referring to the four color components of the optimal SPDs at different CCTs, vary greatly. Peak wavelengths referring to the blue, green, yellow, and red color components vary from 426.1 to 478.7 nm, 500.7 to 532.4 nm, 555.6 to 598.3 nm, and 630.3 to 657.2 nm, respectively. FWHMs referring to the blue, green, yellow, and red color components vary from 20.8 to 50.0 nm, 80.0 to 99.8 nm, 88.3 to 120.0 nm, and 28.3 to 45.0 nm, respectively. In addition, proportions referring to the blue, green, yellow, and red color components vary from 0.46 to 1.00, 0.00 to 1.00, 0.06 to 0.98, and 0.60 to 1.00, respectively. Therefore, it is difficult to realize true seven white LEDs with high color performances at different CCTs by controlling phosphor ingredients, phosphor proportions, and packaging technologies.

As it is feasible and simple to obtain white light by tuning driving currents of the color components [15], we can achieve real white light of high LER and color performance by fabricating an LED module consisting of four color components that can be controlled by driving their currents independently. The LED module is shown in Fig. 3. In this paper, we use the optimal results for CCT=4954 K from Table 1 for our design. The first color component is an InGaN blue chip (450 nm, CREE). The second color component is a phosphor-converted (PC) LED with a blue chip and a high-density green phosphor (525 nm, Intematix G2762), which only emits green fluorescence because its blue light is completely absorbed by its high-density phosphor. Similarly, the third color component is a PC LED with a blue chip and a high-density yellow phosphor (570 nm, Intematix YAG-02). The fourth color component is an InAlGaN red chip (630 nm, CREE).

The SPDs of the four color components at a driving current of 350 mA, $S_b(\lambda)$, $S_g(\lambda)$, $S_g(\lambda)$, and $S_r(\lambda)$, were measured by an integrating sphere spectrometer ATA-1000 (Everfine Inc., China), which offers spectral ranges from 380 to 780 nm and wavelength accuracy of 0.3 nm. All the results are tested at an ambient temperature of 25 °C and shown in Fig. 4(a). As we can see from Fig. 4, the four LEDs are independent, thus no electrical interaction needs to consider. The final white SPD is the result of the color mixing of these four LEDs actually, which can be expressed as

$$S_W(\lambda) = p_b S_b(\lambda) + p_g S_g(\lambda) + p_y S_y(\lambda) + p_r S_r(\lambda), \quad (6)$$

where p_b, p_g, p_y, and p_r are the current proportions of the four color components at a driving current of 350 mA. By recalculation, white light spectra with maximal LER and constrained, high R_a, R_9, and Q_a, can be achieved by varying the current proportions, and the driving currents of each component are 50 mA, 234 mA, 350 mA and 150 mA, respectively. With optimization, we can obtain an LED module with optical power (P_{opt})=579.7 mW, LER=344 lm/W, R_a=90, R_9=98, Q_a=90, and CCT=4439 K. Fig. 4(b) shows the optimal SPD of the LED module. Therefore, white LED modules with high LER, high CRI and CQS can be obtained by our optimization.

4. Conclusions

In this study, we proposed a method to optimize the SPD of an LED module consisting of a blue chip, green and yellow phosphors, and a

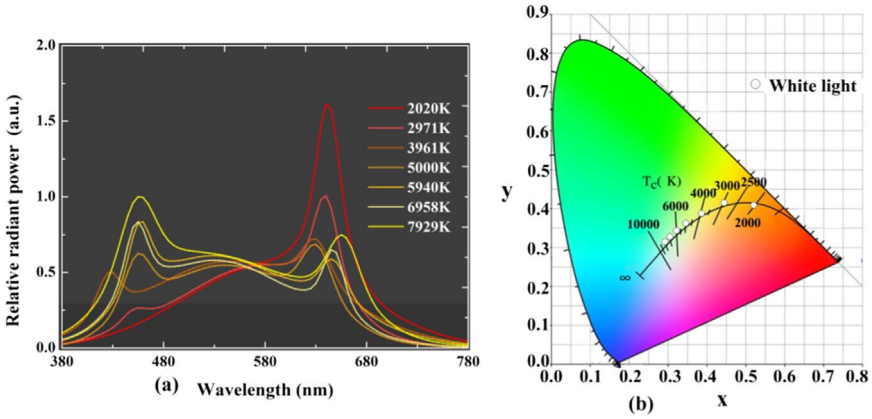

Fig. 2. Optimization results for (a) spectra at CCT from 2020 K to 7929 K and (b) the color coordinates in a CIE 1931 diagram. (For interpretation of the references to color in this figure legend, the reader is referred to the web version of this article.)

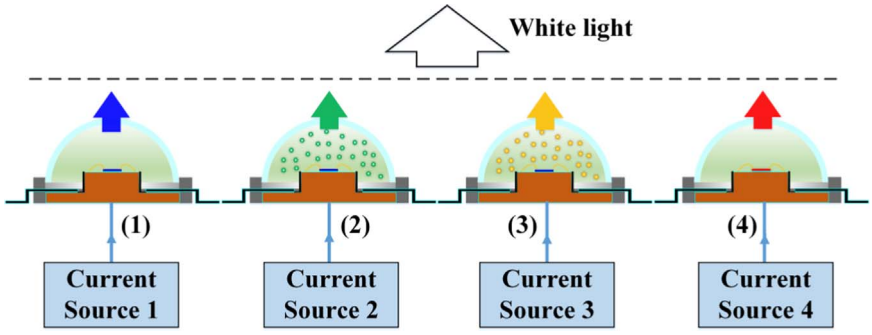

Fig. 3. CCT-tunable LED module. (For interpretation of the references to color in this figure, the reader is referred to the web version of this article.)

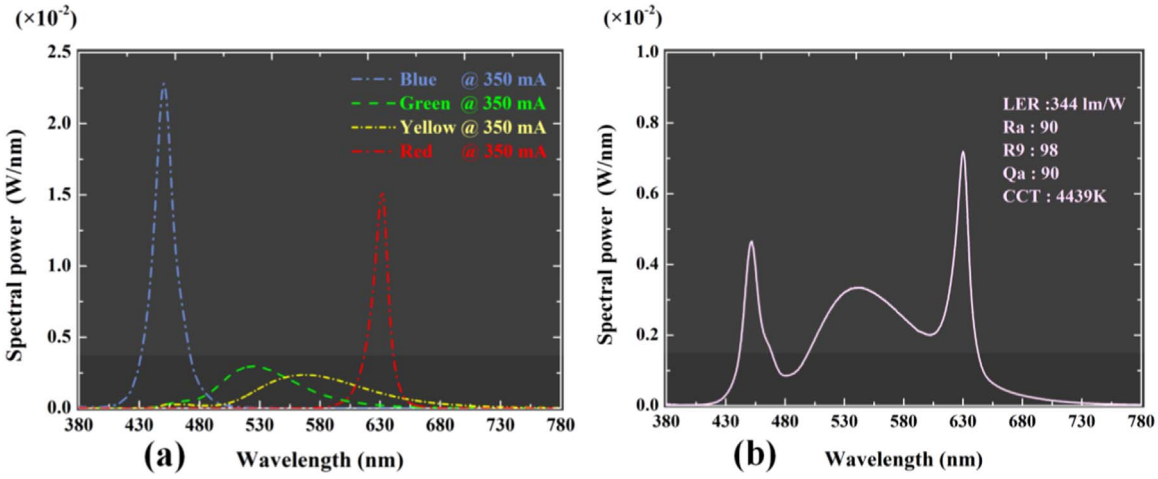

Fig. 4. Optimization results for (a) SPDs of four color components at a driving current of 350 mA and (b) an optimal SPD consisting of four color components when *CCT*=4439 K. (For interpretation of the references to color in this figure legend, the reader is referred to the web version of this article.)

red chip to realize high LER, high CRI and high CQS simultaneously. A GA with a penalty function was developed to optimize the white LED spectra with maximal *LER* and constraints of D_{uv} ≤0.0054, CRI (R_a, R_9)≥95, and CQS (Q_a)≥95. By simulations, the optimal spectra of an LED with high values of CRI and CQS at various CCTs from 2020 K to 7929 K were obtained. LER reached the highest value of 318 lm/W at *CCT*=2996 K. For realizing real white light of high LER and color performance simply, we fabricated an LED module consisting of four color components that can be controlled independently by driving currents. An LED module with *LER*=344 lm/W, R_a=90, R_9=98, Q_a=90, and *CCT*=4439 K was obtained in the experiment. The present method has potential to be well-applied in color mixing to realize the required lighting characteristics.

Acknowledgments

This work was supported by the National Natural Science Foundation of China (Nos. 61604135, 51576078) and the Fundamental Research Funds for the Central Universities, China University of Geosciences (Wuhan) (No. CUGL 150848).

References

[1] H. Amano, N. Sawaki, I. Akasaki, Y. Toyoda, Metalorganic vapor-phase epitaxial-growth of a high-quality GaN film using an AlN buffer layer, Appl. Phys. Lett. 48 (5) (1986) 353–355.
[2] E.F. Schubert, Light Emitting Diodes, 2nd ed., Cambridge University Press, Cambridge, UK, 2006.

[3] E.F. Schubert, J.K. Kim, Solid-state light sources getting smart, Science 308 (5726) (2005) 1274–1278.
[4] Commission Internationale de l'Eclairage, Method of measuring and specifying colour rendering properties of light sources, Technical Report CIE 013.3, 1995.
[5] Commission Internationale de l'Eclairage, Color rendering of white LED light sources, Technical Report CIE 177, 2007.
[6] Y. Ohno, Spectral design considerations for color rendering of white LED sources, Opt. Eng. 44 (11) (2005) 111302.
[7] W. Davis, Y. Ohno, Color quality scale, Opt. Eng. 49 (3) (2010) 033602.
[8] N. Pousset, O. Galël, A. Razet, Visual experiment on LED lighting quality with color quality scale colored samples, CIE 2010: Lighting Quality and Energy Efficiency, Vienna, Austria, 2010.
[9] J.H. Oh, Y.J. Eo, S.J. Yang, Y.R. Do, High-color-quality multipackage phosphor-converted leds for yellow photolithography room lamp, IEEE Photonics J. 7 (2) (2015) 1300308.
[10] T. Erdem, Y. Kelestemur, Z. Soran-Erdem, Y. Jin, H.V. Demir, Energy-saving quality road lighting with colloidal quantum dot nanophosphors, Nanophotonics 3 (6) (2014) 373–381.
[11] H.T. Li, X.L. Mao, Y.J. Han, Y. Luo, Wavelength dependence of colorimetric properties of lighting sources based on multi-color LEDs, Opt. Express 21 (3) (2013) 3775–3783.
[12] J.H. Oh, H. Kang, Y.J. Eo, H.K. Park, Y.R. Do, Synthesis of narrow-band red-emitting K2SiF6: Mn4+ phosphors for a deep red monochromatic led and ultrahigh color quality warm-white LEDs, J. Mater. Chem. C 3 (3) (2015) 607–615.
[13] Q. Dai, L. Hao, Y. Lin, Z. Cui, Spectral optimization simulation of white light based on the photopic eye-sensitivity curve, J. Appl. Phys. 119 (5) (2016) 053103.
[14] K.A. Bulashevich, A.V. Kulik, S.Y. Karpov, Optimal ways of colour mixing for high-quality white-light LED sources, Phys. Status Solidi A 212 (5, SI) (2015) S914–S919.
[15] P. Zhong, G. He, M. Zhang, Spectral optimization of the color temperature tunable white light-emitting diode (LED) cluster consisting of direct-emission blue and red LEDs and a diphosphor conversion LED, Opt. Express 20 (19) (2012) A684–A693.
[16] Wendy Davis, Yoshi Ohno, Development of a Color Quality Scale, National Institute of Standards and Technology, Gaithersburg, US, 2005.
[17] C. Sommer, F.P. Wenzl, P. Hartmann, P. Pachler, M. Schweighart, S. Tasch, G. Leising, Tailoring of the color conversion elements in phosphor-converted high-power LEDs by optical simulations, IEEE Photonics Technol. Lett. 20 (9) (2008) 1041–1135.
[18] H. Jin, S. Jin, K. Yuan, S. Cen, Two-part gauss simulation of phosphor-coated LED, IEEE Photonics J. 5 (4) (2013) 1600110.
[19] Y. Lin, Z. Deng, Z. Guo, Z. Liu, H. Lan, Y. Lu, Y. Cao, Study on the correlations between color rendering index and the spectral power distribution, Opt. Express 22 (S4) (2014) A1029–A1039.
[20] K. Deb, An efficient constraint handling method for genetic algorithms, Comput. Method Appl. Mech. 186 (2–4) (2000) 311–338.
[21] P. Zhong, G. He, M. Zhang, Optimal spectra of white light-emitting diodes using quantum dot nanophosphors, Opt. Express 20 (8) (2012) 9122–9134.